Topography of Visuomotor Parameters in the Frontal and Premotor Eye Fields

Helen E. Savaki[1,2], Georgia G. Gregoriou[1,2], Sophia Bakola[1] and Adonis K. Moschovakis[1,2]

[1]Institute of Applied and Computational Mathematics, Foundation for Research and Technology Hellas, GR-71110 Iraklion, Crete, Greece and [2]Faculty of Medicine, Department of Basic Sciences, School of Health Sciences, University of Crete, GR-71003 Iraklion, Crete, Greece

Address correspondence to Helen E. Savaki, Faculty of Medicine, Department of Basic Sciences, School of Health Sciences, University of Crete, GR-71003 Iraklion, Crete, Greece. Email: savaki@med.uoc.gr

To determine whether the periarcuate frontal cortex spatially encodes visual and oculomotor parameters, we trained monkeys to repeatedly execute saccades of the same amplitude and direction toward visual targets and we obtained quantitative images of the distribution of metabolic activity in 2D flattened reconstructions of the arcuate sulcus (As) and prearcuate convexity. We found two topographic maps of contraversive saccades to visual targets, separated by a region representing the vertical meridian: the first region straddled the fundus of the As and occupied areas 44 and 6-ventral, whereas the second one occupied areas 8A and 45 in the anterior bank of the As and the prearcuate convexity. The representation of the vertical meridian runs along the posterior borders of areas 8A and 45 (deep in the As). In both maps, the upper part of visuo-oculomotor space is represented ventrally and laterally and the lower part dorsally and medially whereas dorsal and ventral regions are separated by the representation of the horizontal meridian.

Keywords: visuo-oculomotor space, areas 6v 8a 44 45, FEF; premotor cortex, visually guided saccades

Introduction

Because of its relative simplicity, the oculomotor system has been the object of extensive efforts to understand how the brain specifies movement variables. Saccade metrics are determined by a neural circuit, which comprises several classes of neurons distributed through several brain regions. Premotoneurons of the reticular formation are known to use a time code to specify saccade amplitude and direction (Moschovakis et al. 1996). Higher-order structures such as the superior colliculus use a place code to represent the vector of desired saccades. Cells that prefer small saccades are located in the rostral part of the colliculus, and cells preferring large saccades are located more caudally, whereas cells preferring upward saccades are located medially and cells preferring downward saccades are located laterally (Sparks et al. 1976). It is less clear how the frontal eye field (FEF) uses neural space to represent variables related to visually guided eye movements.

Microstimulation studies helped designate a low-threshold FEF in the monkey brain in the anterior bank of the arcuate sulcus (As) (Bruce et al. 1985). It partially overlaps two cytoarchitectonically defined regions of the frontal lobes, areas 8A and 45 of Walker (Walker 1940). The former occupies the superficial half of the anterior wall of the superior limb of the As and the exposed surface close to it, whereas the latter occupies the rostral bank of the inferior limb of the As and the exposed surface close to it. In addition to these, a more extended FEF encompassing some of the premotor cortical area 6 is suggested by neurophysiological, neuroanatomical, and functional imaging studies (Fujii et al. 1998; Moschovakis et al. 2004; Baker et al. 2006; Amiez and Petrides 2009). Within the classical FEF in the anterior bank of the As, small saccades are represented laterally and ventrally toward its inferior limb and large saccades are represented medially and dorsally toward its superior limb (Bruce et al. 1985; Sommer and Wurtz 2000). No topographic map of saccade amplitudes or directions has been found in the more extended FEF. The present report is part of a long-term effort to understand how neural space is used to encode saccade metrics (Moschovakis et al. 2001, 2004; Bakola et al. 2007; Savaki et al. 2010). Here, to examine whether populations of FEF neurons encode visual and oculomotor parameters in terms of their location in the FEF, we used the [14C] deoxyglucose (14C-DG) quantitative autoradiographic method (Sokoloff et al. 1977; Savaki et al. 1980) to obtain images of their aggregate activity in rhesus monkeys repeatedly performing saccades of the same amplitude and direction to visual targets. We wish to emphasize that FEF neurons generally discharge for visual stimuli with or without saccades and few cells discharge before spontaneous saccades in the dark (Goldberg and Bushnell 1981; Bruce and Goldberg 1985). Accordingly, the presentation of visual targets was chosen as the most effective means to drive saccades and activate the region we wanted to study. The disadvantage is that we cannot be certain that the activations documented represent oculomotor space, visual space, or both.

Materials and Methods

Subjects and [14C]-DG Experiments

Ten head-fixed adult female monkeys (*Macaca mulatta*) weighing between 3 and 5 kg were used in experimental protocols complying with European Union directive 86/609 and approved by the Animal Use Committee of FO.R.T.H. Surgical procedures were performed under general anesthesia (sodium pentobarbital, 25 mg/kg i.m.) and aseptic conditions. A metal bolt was cemented onto mandibular plates secured on the cranium with titanium screws for head immobilization. Search coils were sutured on the sclera to record the instantaneous eye position, which was digitized at a rate of 500 Hz using the Spike2 software (Cambridge Electronics Design) as described earlier (Moschovakis et al. 2001). All tasks were performed without ambient illumination. Targets were presented on a video screen (23 cm in front of the animal) as red circles of 1.5° in diameter, and monkeys were required to hold eye position within a circular window of 2.5° in diameter surrounding each target. Successful completion of each trial was rewarded with water delivered via a tube attached close to the mouth of the animal. Monkeys were trained for 1 h per day during 3–6 months until they perfected their performance (95% success rate). The 14C-DG experiments, the preparation of autoradiograms, the quantitative densitometric analysis, and the calculation of local cerebral glucose utilization (LCGU) values were performed as previously described (Gregoriou and Savaki 2001; Savaki et al. 2010). Briefly, each monkey was

subjected to femoral vein and artery catheterization under general anesthesia and was allowed 4–5 h to recover. Five minutes after initiation of task performance, the tracer (100 Ci/kg of 2-deoxy-D-1-^{14}Cglucose of specific activity 55 mCi/mmol) was injected intravenously, and arterial samples were collected from the femoral artery during the next 45 min as per the original description of the method (Sokoloff et al. 1977). These arterial blood samples were used to measure plasma ^{14}C-DG and glucose concentrations. At 45 min, the monkey was killed by intravenous injections of 50 mg of sodium thiopental in 5 mL of saline and then a saturated potassium chloride solution. The brain was removed, frozen in isopentane at −50°C, and stored at −80°C. Each hemisphere of each monkey was cut horizontally in a cryostat at −20°C to obtain a total of ~950 serial sections, 20 micron thick, covering the dorsoventral extent of the As. The adjacent horizontal sections were exposed with medical X-ray films, together with precalibrated ^{14}C-standards, to prepare autoradiographs. Intermediate sections were used for Nissl staining. The LCGU values (in μmol/100 g/min) were calculated from the local ^{14}C tissue concentration (densitometrically determined from the autoradiographs) and the plasma ^{14}C and glucose concentrations, according to the operational equation and the appropriate kinetic constants for the monkey (Sokoloff et al. 1977; Kennedy et al. 1978). Normalization of LCGU values was based on the averaged unaffected gray matter value pooled across all monkeys, as described earlier (Savaki et al. 2010).

Tasks

Control Tasks

Three monkeys served as controls. Two monkeys were trained to fixate a central fixation point (control-fixation, Cf), and one monkey was free to move its eyes in the dark (control-dark, Cd). The Cf monkeys maintained fixation of a central visual target located straight ahead for the duration of the trial (4 s). Intertrial intervals were 0.2–0.3 s long. These monkeys maintained fixation for 75–80% of the ^{14}C-DG experiment. The Cd monkey was seated in the dark (Cd) in front of the idle apparatus and received reward at random intervals, so that the total number of rewards matched that of monkeys rewarded for executing saccades.

Saccade Tasks

Seven monkeys served as experimental animals to study the representation of visuo-oculomotor space in the arcuate and prearcuate cortex. Two monkeys were trained to execute horizontal saccades, one made vertical saccades, and four monkeys made oblique upward and/or downward saccades to visual targets (Table 1, Fig. 1). Most of these monkeys were also used to study the place code of saccade metrics in the cortex of the lateral intraparietal sulcus (Savaki et al. 2010). One of the two monkeys executing horizontal saccades to visual targets was required to perform a sequence of 5°, 10°, and 15° movements to the left, followed by two consecutive 30° movements to the right and a 30° movement to the left in each trial. Each trial was initiated with the appearance of a central fixation target. The monkey had to fixate on the central visual target until it disappeared and another target was illuminated signaling that a saccade should be executed within 1 s. The minimum latency to move the eyes after onset of each target was set to 0.1 s to discourage anticipatory movements. The monkey was required to fixate each visual target for 0.3–0.6 s until it disappeared. Intertrial intervals ranged between 0.5 and 0.8 s. Only the right hemisphere of this monkey (contralateral to the 5°, 10°, 15°, and 30° leftward saccades) was used to study the representation of the horizontal meridian. The second monkey executing visually guided saccades along the horizontal meridian was required to perform a sequence of 5°, 10°, and 15° movements to the left, followed by a 30° movement to the right, then a sequence of 5°, 10°, and 15° movements to the right, followed by a 30° movement to the left in each trial. Both hemispheres of this monkey were used to study the representation of the horizontal meridian in FEF. The third monkey was asked to execute vertical saccades to visual targets. This monkey was required to perform a sequence of 5°, 10°, and 15° upward movements, followed by a 30° downward movement, then a sequence of 5°, 10°, and 15° downward movements, followed

Table 1

Metrics and number of task-related saccades contraversive to the hemispheres under analysis

	Saccade direction per trial		Saccade amplitude (degrees)	Number of saccades
Monkey 1	Horizontal left	←	5	127
	Horizontal left	←	10	111
	Horizontal left	←	15	112
	Horizontal left	←	30	100
Monkey 2	Horizontal left	←	5	72
	Horizontal left	←	10	53
	Horizontal left	←	15	61
	Horizontal left	←	30	62
	Horizontal right	→	5	90
	Horizontal right	→	10	75
	Horizontal right	→	15	67
	Horizontal right	→	30	50
Monkey 3	Vertical up	↑	5	74
	Vertical up	↑	10	74
	Vertical up	↑	15	65
	Vertical up	↑	30	63
	Vertical down	↓	5	105
	Vertical down	↓	10	81
	Vertical down	↓	15	63
	Vertical down	↓	30	62
Monkey 4	Oblique up left	↖	20	119
Monkey 5	Oblique down right	↘	10	212
Monkey 6	Oblique up left	↖	20	130
	Oblique down right	↘	10	331
Monkey 7	Oblique up left	↖	10	323
	Oblique down right	↘	20	156

Note: Behavioral tasks: Monkey 1 performed a full sequence of 5°, 10°, and 15° visually guided saccades to the left from the central fixation point, followed by two consecutive 30° saccades to the right and a 30° saccade to the left, along the horizontal meridian, in each trial. Only the task-related saccades (leftward saccades contraversive to the studied right hemisphere) are presented in the table. Monkey 2 executed a sequence of 5°, 10°, and 15° visually guided saccades to the left, followed by a 30° saccade to the right, then a sequence of 5°, 10°, and 15° saccades to the right, followed by a 30° saccade to the left, along the horizontal meridian, in each trial. Monkey 3 performed a sequence of 5°, 10°, and 15° visually guided upward saccades from the central fixation point, followed by a 30° downward saccade, then a sequence of 5°, 10°, and 15° downward saccades, followed by a 30° upward saccade, along the vertical meridian, in each trial. Monkey 4 executed a visually guided oblique saccade 20° up–left from the central fixation point in the direction of 135° in each trial and was free to move its eyes spontaneously during the intertrial interval. Monkey 5 performed a sequence of two down–right visually guided saccades from the central fixation point 10° in amplitude and 315° in direction and was free to move its eyes spontaneously during the intertrial interval. Monkey 6 executed a sequence of a 20° up–left visually guided saccade (135° direction) followed by two down–right 10° saccades (315° direction) in each trial. Monkey 7 performed a sequence of two 10° up–left saccades (135° direction) followed by one 20° down–right saccade (135° direction) in each trial. The column titled "Saccade Direction per trial" refers only to saccades contraversive to each studied hemisphere. Direction of saccades is represented by black arrow. The column titled "Number of Saccades" refers to the total number of saccades each monkey executed to each direction during the critical 10 first min of the ^{14}C-DG experiment.

by a 30° upward movement. Task parameters were the same as in the previous case. Both its hemispheres were used to study the representation of the vertical meridian in FEF. The fourth monkey was required to execute oblique up–left saccades to visual targets located 20° away from the central fixation point in the direction of 135°. This monkey had to fixate each target for 0.5–1 s until it disappeared. The animal was free to move its eyes spontaneously during the intertrial interval (1–1.8 s). The endpoints of the rightward saccades of this animal were dispersed so that the left FEF would not be activated and the right FEF would not be influenced. Thus, only its right hemisphere was used to
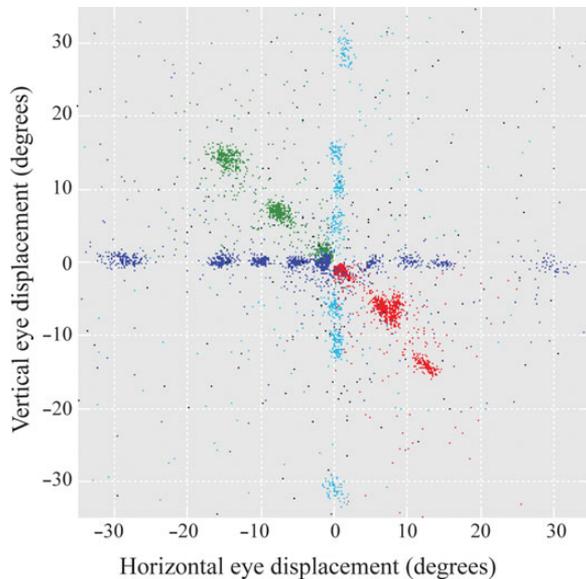
Figure 1. Scatterplots of the horizontal (abscissa) and vertical (ordinate) eye displacements (in degrees) of all saccades executed by the seven experimental monkeys we studied during the critical first 10 min of the ^{14}C-DG experiment. Dark blue dots represent horizontal, light blue dots vertical, green dots oblique upward, and red dots oblique downward saccades to visual targets. Moreover, black dots represent the saccades executed by the control in the dark (Cd) monkey.

study the representation of saccades to visual targets (in this case upward oblique). For the same reason, only the left hemisphere was used from the fifth monkey, which had to perform a sequence of two down–right visually guided saccades 10° in amplitude and 315° in direction in each trial. The sixth monkey had to execute a sequence of a 20° up–left saccade (135° direction) followed by two down–right 10° saccades (315° direction) in each trial, thus contributing one hemisphere contralateral to oblique up and one contralateral to oblique down saccades to visual targets. With the exception of the intertrial interval (0.5–1 s), task parameters were the same as in the previous case. The same was true of the seventh monkey that was required to perform a sequence of two 10° up–left saccades (135° direction) followed by one 20° down–right saccade (135° direction) in each trial.

Reconstruction of Cortical Maps

The spatio-intensive pattern of metabolic activity within the anteroposterior and dorsoventral extents of the As in each hemisphere was reconstructed in two-dimensional (2D) maps as previously described in other cortical areas (Gregoriou and Savaki 2003; Savaki et al. 2010). Briefly, for each 20-μm-thick horizontal section through the As, LCGU values were measured (pixel by pixel, at a resolution of 50 μm/pixel) along a line parallel to the surface of the cortex (Fig. 2A, Sections 1, 2, gray area abcd), covering the entire thickness of the cortical gray matter (all cortical layers). Each data array (a series of LCGU values in each horizontal section) was aligned with the arrays obtained from adjacent sections, on the anterior tip of the floor of the As (dorsal sections, Fig. 2A1, point c), or the fundus of the sulcus (ventral sections, Fig. 2A2, point c). To reconstruct the periarcuate eye field map, the dorsoventral plotting resolution was set to 100 μm. Accordingly, each line of the 2D reconstructed metabolic maps (Figs 3–5) represents the distribution of metabolic activity averaged over five adjacent horizontal sections. The same plotting resolution used for the dorsoventral axis (100 μm) was also adopted for the anteroposterior axis of the 2D-reconstructed maps.

The size of each cytoarchitectonically identified cortical area varied considerably from hemisphere to hemisphere. To quantify the amount of variability in the location of the surface landmarks and cytoarchitectonic borders, we calculated the standard deviation (SD) of the anteroposterior position of each border relative to the point of alignment.
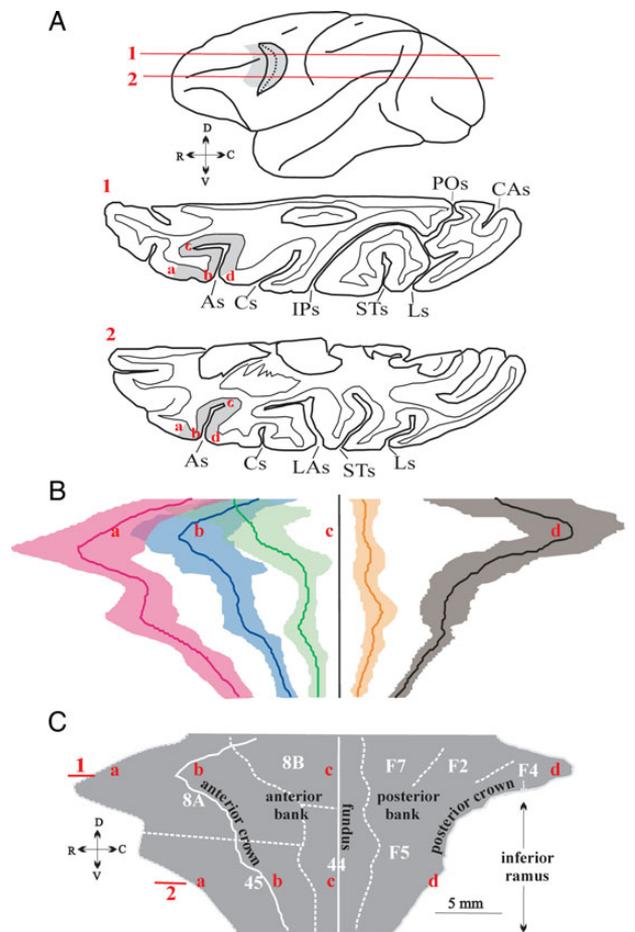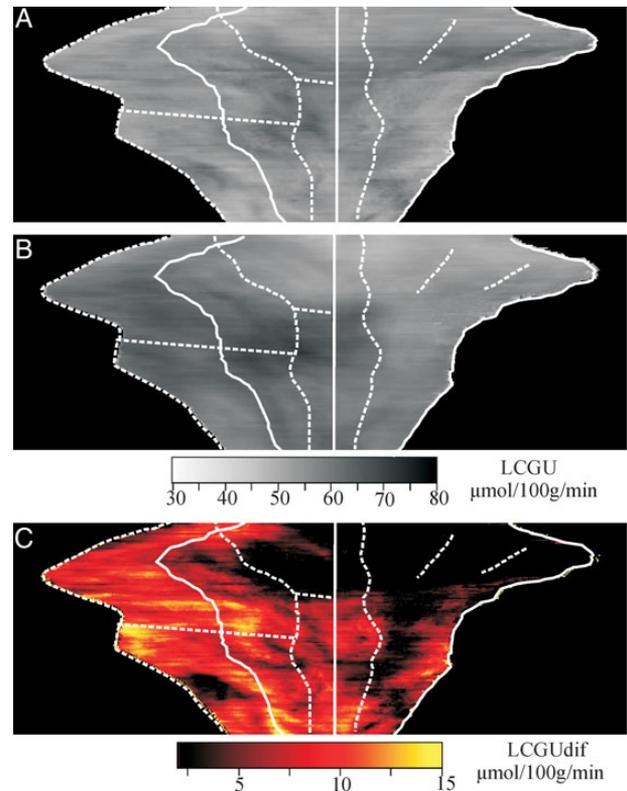

Figure 2. Two-dimensional reconstruction of the cortex lying in the As and the prearcuate convexity. (A) Schematic representation of two horizontal sections (1 and 2) passing through the left hemisphere at the dorsoventral level indicated on this lateral view of the brain. The gray area (marked with the red letters a through d in A1, 2) indicates the portion of the As and prearcuate convexity that was flattened. Red letters indicate: the anterior border of area 8A (in Section 1) and area 45 (in Section 2) in the frontal convexity (a), the crown of the anterior bank of the As (b), the fundus of the As (c), and the crown of the posterior bank of the As (d). As, arcuate sulcus; Cs, central sulcus, CAs, calcarine sulcus; IPs, intraparietal sulcus; Ls, lunate sulcus, Las, lateral sulcus, POs, parieto-occipital sulcus, Ps, principal sulcus, STs, superior temporal sulcus. (B) Average map of the unfolded As and the prearcuate convexity. Shading represents mean position for each border ± 1 SD calculated from all hemispheres we studied ($n = 17$) aligned on the fundus of As. Top corresponds to dorsal sections, bottom to ventral sections, left to anterior, and right to posterior sites. Magenta depicts the anterior border of area 8A dorsally and 45 ventrally. Blue: anterior crown of As. Green: posterior border of 8A dorsally and 45 ventrally. Orange: anterior border of F7 dorsally and F5 ventrally. Black: posterior crown of As. Letters a–d (in red) indicate the same landmarks as in A and C. (C) Geometrically normalized 2D map of the unfolded As and the prearcuate convexity. Numbers 1, 2 (in red) indicate the dorsoventral location of the sections drawn in A. Solid vertical line indicates the fundus of the As, which was used as the point of alignment of adjacent sections. The part of the reconstruction to the right of the fundus corresponds to the posterior bank of the sulcus harboring premotor areas F2, F7 dorsally, and F5 ventrally. Cytoarchitectonically identified areas 8A and 8B dorsally and area 45 ventrally in the anterior bank of the As and the prearcuate convexity are also shown. Dotted white lines indicate the cytoarchitectonically identified borders of the anatomical areas indicated. Solid white lines indicate surface landmarks, that is, the crowns and fundus of the As. C, caudal; D, dorsal; R, rostral; V, ventral.

The mean position of each border (average map to which all different maps were normalized) ± 1 SD is shown in Figure 2B. To compensate for this variability and allow direct comparison of the sites of activation in the FEF of different hemispheres, individual 2D maps were geometrically normalized around their cytoarchitectonically identified borders
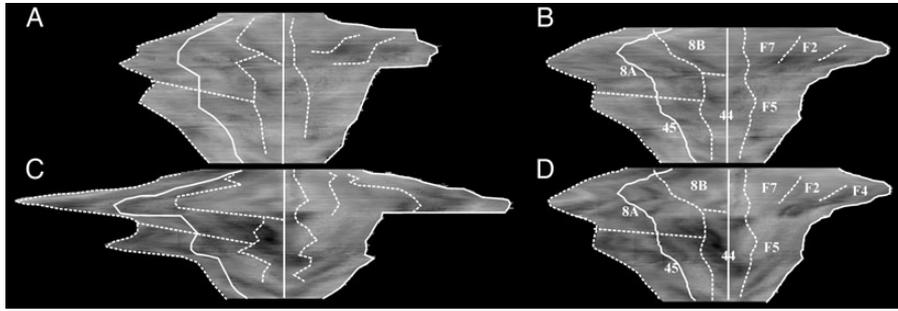
Figure 3. Examples of geometrically normalized 2D maps of the unfolded As and the prearcuate convexity. Maps reconstructed from one hemisphere with small (A,B) and one hemisphere with large (C,D) spur, before (A,C) and after (B,D) geometrical normalization. Map A corresponds to one of the Cd hemispheres and map C to a hemisphere representing the vertical meridian.

and crowns of the As. To this end, we first calculated the average dorsoventral extent of areas 8A and 45 (Fig. 2B, 8A/45 border in yellow). The LCGU data from each map were subsequently resampled along the dorsoventral dimension using linear interpolation so that in all maps the dorsoventral lengths of areas 8A and 45 were equal to the average dorsoventral extent of each of the two areas. Moreover, individual metabolic maps were normalized along the anteroposterior dimension so that the extent of each cortical area and the relative position of surface landmarks (crowns and fundus of the As) and cytoarchitectonic borders was the same in all maps. To this end, in the dorsal sections at each dorsoventral level, we measured the distances between: (1) the anterior border of area 8A (Fig. 2B, magenda line, a) and the anterior crown of As (Fig. 2B, blue line, b), (2) the latter and the posterior border of 8A (Fig. 2B, green line), (3) the latter and the fundus (Fig. 2B, straight black line, c), (4) the fundus and the anterior border of F7 (Fig. 2B, orange line), (5) the anterior and the posterior border of F7 (Fig. 2C), and (6) the latter and the posterior crown of the As (Fig. 2B, black line, d). Similarly, in the ventral sections, we measured the distances between: (1) the anterior border of area 45 (Fig. 2B, magenda line, a) and the anterior crown of the As (Fig. 2B, blue line, b), (2) the latter and the posterior border of 45 (Fig. 2B, green line), (3) the latter and the fundus, (4) the fundus and the posterior border of 44 (Fig. 2B, orange line), and (5) the latter and the posterior crown of the As. The average of each one of these lengths was separately calculated from all hemispheres to construct a reference surface landmark map (Fig. 2C). The 2D map of each hemisphere was then fit to this reference map by stretching or compressing the length of each line between two adjacent landmarks at each dorsoventral level to fit the respective distances in the reference map with the help of custom-designed routines in the Matlab environment (Mathworks) (Gregoriou et al. 2005). In this manner, we generated a geometrically normalized map of the periarcuate cortex containing a standard number of pixels. Two typical examples of reconstructed maps before (A and C) and after (B and D) geometrical normalization are provided in Figure 3. The first one corresponds to a hemisphere with a small spur (Fig. 3A) whereas the second one represents a hemisphere with a large spur (Fig. 3C). Data from different geometrically normalized maps were combined to obtain average metabolic maps and the difference between them. To generate average maps, the LCGU value found in a certain pixel in one of the geometrically normalized maps was added to the value found in the pixel occupying the same position in other maps of the same group of animals, and the result was divided by the number of maps analyzed (Fig. 4A,B; Fig. 5A–E). To generate a difference map, the LCGU value found in a certain pixel of a geometrically normalized map of a control hemisphere was subtracted from the value found in the pixel occupying the same position in a similar map obtained from an experimental animal (Fig. 4C). To generate maps summarizing the topography of direction of visually guided saccades in the periarcuate eye field, we generated reconstructions in which all pixels displaying activity higher than 10% relative to the corresponding pixels of the control map are shown in a different color for different directions of movement (Fig. 6A–D), and then, we superimposed them in a single map (Fig. 6E). Percent LCGU differences between experimental and control
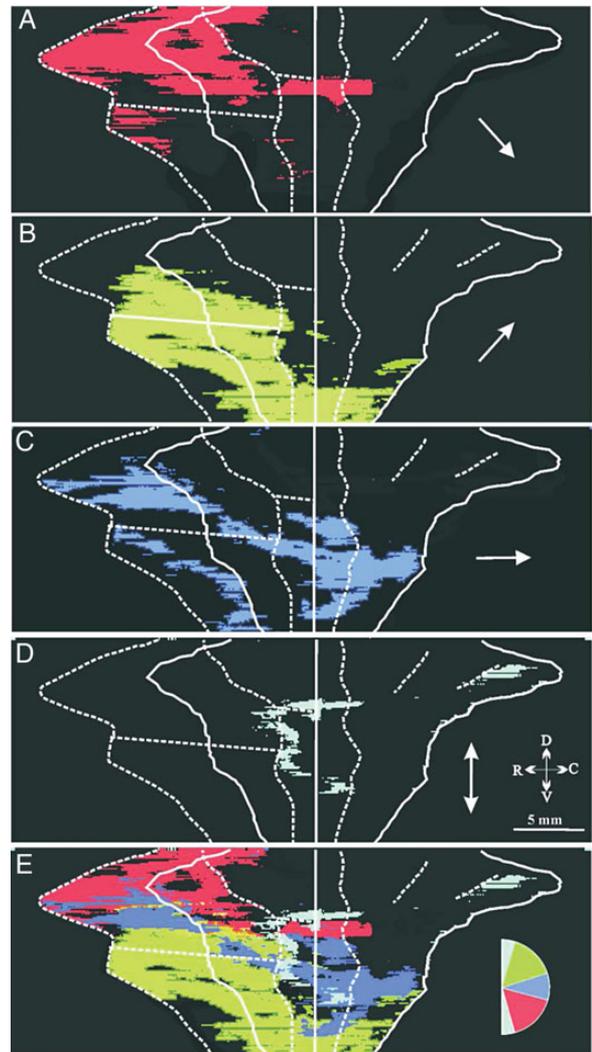

Figure 4. Two-dimensional reconstructed maps of LCGU values (μmol/100 g/min) in the unfolded As and the prearcute convexity. (A) Quantitative 2D map of metabolic activity obtained after averaging the LCGU values, pixel by pixel, in the geometrically normalized maps of both hemispheres of the Cd monkey. White lines represent anatomical boundaries and surface landmarks as indicated in Figure 2C. (B) Average quantitative 2D map obtained from all hemispheres of all experimental monkeys, including those executing fixation, horizontal, upward, downward, and vertical saccades to visual targets. Gray-scale bar indicates LCGU values in micromoles per 100 g per minute and also applies to (A). (C) Quantitative 2D map of metabolic activity generated after subtracting the average Cd map (A) from the average saccade-related map shown in B. Color bar indicates LCGU difference from the Cd monkey in μmoles/100 g/minute.

subjects were calculated as (experimental − control) × 100/control. Table 2 demonstrates comparisons between the experimental groups and the Cf and Cd, respectively (%Cf and %Cd). For example, to estimate the effect in the representation of the HM, we first subtracted the average control map from the average map of monkeys executing horizontal saccades. This subtraction revealed a significant activation in the area represented by dark blue in Figure 6C, which corresponds to the
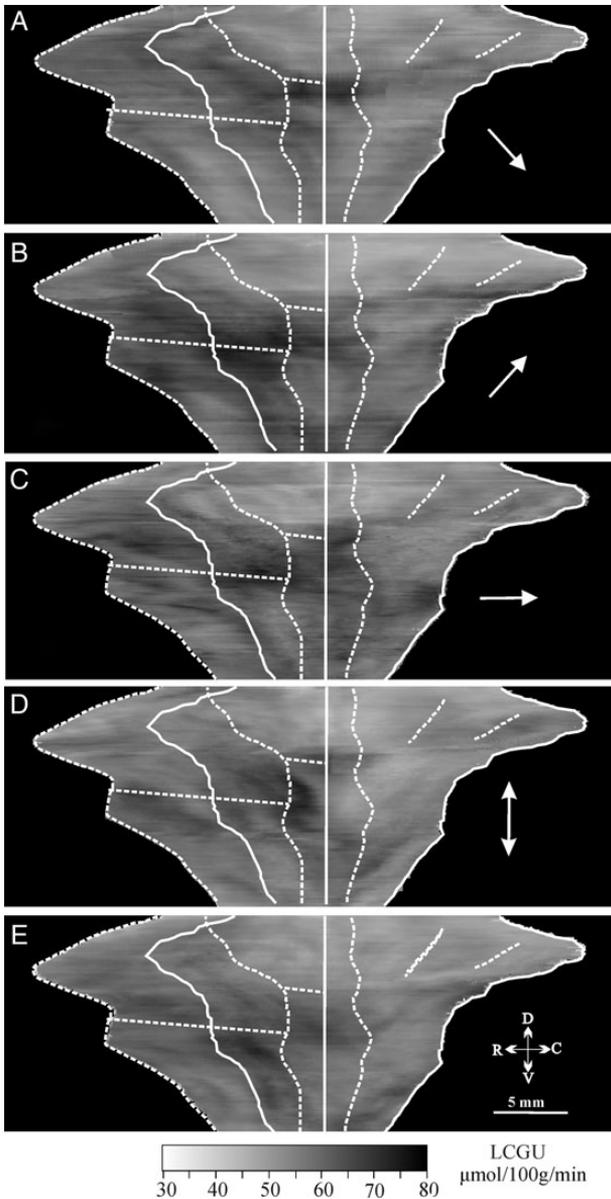
Figure 5. Two-dimensional reconstructions of the distribution of metabolic activity elicited by saccades of different directions. (*A*) Map averaged from the three hemispheres of the monkeys executing contraversive oblique down saccades. (*B*) Map averaged from the three hemispheres of the monkeys executing contraversive oblique up saccades. (*C*) Map averaged from three hemispheres of monkeys executing contraversive horizontal saccades. (*D*) Map averaged from the two hemispheres of a monkey executing vertical up and down saccades. (*E*) Map averaged from the four hemispheres of the two fixating monkeys (Cf). The gray-scale bar indicates LCGU values in μmoles/100 g/minute. The white arrow in each panel demonstrates the direction of saccades to visual targets executed by the animals contributing to the map illustrated.

Figure 6. Representation of visuo-oculomotor space in the periarcuate frontal cortex. (*A*) Pixels of the map averaged from the hemispheres contralateral to oblique down saccades (red), displaying LCGU values 10% higher than the corresponding ones of the Cd map. (*B*) Similarly for contralateral oblique up saccades (green), horizontal saccades (dark blue, *C*) and vertical saccades (light blue, *D*). (*E*) Superimposition of the areas activated for downward (red), upward (green), horizontal (dark blue), and vertical (light blue) saccades shown in *A–D*.

Moreover, we analyzed LCGU differences of >10% relative to the corresponding control values, a conservative criterion considering the fact that the maximum inter-hemispheric difference in normal awake monkeys is 7% (Kennedy et al. 1978; Raos et al. 2007; Savaki et al. 2010).

Results

Oculomotor Behavior

Seventeen hemispheres from 10 monkeys were analyzed to study the representation of visual and oculomotor space in the arcuate and prearcuate cortex. Because the FEF is known to represent the contralateral half of visual space and its microstimulation to evoke contraversive saccades (Bruce and Goldberg 1985; Bruce et al. 1985), we report visually guided saccades contraversive to the hemispheres we studied (Table 1). The first monkey executed 127, 111, 112, and 100 leftward

representation of the HM in the periarcuate cortex. Then, to estimate the activity in the HM of all different groups, we measured the average LCGU within this area in each group. These measurements gave us the values of the first line of Table 2, that is, the LCGU within the cortical area representing the HM in each group of monkeys. In this first line, one can see that the only group displaying a significant increase of activity within the cortical area representing the HM is the group executing horizontal saccades (15.3% and 20.6% increase compared with the Cf and Cd, respectively). To determine statistical significance, we used Student's unpaired *t*-test and rejected the null hypothesis if $P < 0.001$, as well as one-way ANOVA followed by Dunnett's post hoc test to correct for multiple pair-wise comparisons with control monkeys.

Table 2
Effects of visually guided saccades of different directions in the periarcuate cortex

Cortical area representing (n)	Cf	Cd	Down	D %Cf	D %Cd	Up	U %Cf	U %Cd	Horizontal	H %Cf	H %Cd	Vertical	V %Cf	V %Cd
Horizontal meridian (99)	57.4 ± 1.7	54.9 ± 1.6	58.8 ± 4.3	2.4	7.1	60.0 ± 2.9	4.5	9.3	66.2 ± 2.2	**15.3***	**20.6***	60.3 ± 2	5.1	9.8
Vertical meridian (70)	59.8 ± 3.5	59.2 ± 2.4	61.5 ± 2.8	2.8	3.9	62.8 ± 6.2	5.0	6.1	60.2 ± 6.6	0.7	1.7	70.5 ± 4.5	**17.9***	**19.1***
Upper visual space (118)	58.9 ± 1.8	54.1 ± 1.1	57.0 ± 2.0	−3.2	5.4	66.5 ± 2.1	**13.0***	**22.9***	59.9 ± 1.3	1.7	10.7	60.2 ± 2.1	2.3	**11.3***
Lower visual space (64)	55.7 ± 2.6	53 ± 2.6	63.0 ± 3	**13.1***	**18.9***	57.7 ± 3.3	3.6	8.9	57.8 ± 3	3.8	9.1	57.6 ± 2.7	3.4	8.6
Area 8B (64)	54.6 ± 2.6	55.8 ± 3.8	56.8 ± 5.3	3.9	1.8	54.9 ± 3.9	0.5	−1.6	55.1 ± 5.7	0.9	−1.3	58.6 ± 5	7.3	5.0
Premotor cortex F7 (40)	52.5 ± 1.2	54.4 ± 2.5	53.1 ± 2.2	1.1	−2.4	49.6 ± 2.1	−5.5	−8.8	51.2 ± 2.2	−2.5	−5.9	53.1 ± 1.1	1.1	−2.4
Premotor area F2 (41)	52.6 ± 2.3	55.6 ± 3.5	53.6 ± 2.4	1.9	−3.6	51.8 ± 4.2	−1.5	−6.8	54 ± 2	2.7	−2.9	56.2 ± 3.9	6.8	1.1
Premotor area F5 (100)	58.5 ± 4.0	54 ± 1.4	55.9 ± 3.3	−4.4	3.5	61.4 ± 3.7	4.9	**13.7***	61.4 ± 4.1	4.9	**13.7***	59.2 ± 2.8	1.2	**9.6***

Note: LCGU values (mean ± SD in micromoles per 100 g per minute) in different regions of the As and the prearcuate convexity of monkeys executing oblique down (D), oblique up (U), horizontal (H), and vertical (V) saccades to visual targets. The number in parentheses is the number of sets of five adjacent horizontal sections used to measure mean LCGU values in the regions indicated in the leftmost column.

%Cf and %Cd, percent differences relative to Cf and Cd values, measured as (experimental-Cf) *100/Cf and (experimental-Cd)*100/Cd, respectively. Values in bold marked with an asterisk indicate statistically significant differences tested with Student's unpaired t-test ($P < 0.001$) and with one-way ANOVA followed by Dunnett's post hoc test to correct for the fact that control monkeys were used in several pair-wise comparisons.

horizontal saccades of 5°, 10°, 15°, and 30° amplitude, respectively, as well as 191 rightward horizontal saccades of 30° amplitude, within the critical first 10 min of the experiment. A second monkey executed 72, 53, 61, and 62 leftward horizontal saccades of 5°, 10°, 15°, and 30° amplitude, respectively, as well as 90, 75, 67, and 50 rightward horizontal saccades of the same amplitudes. Both hemispheres of the second monkey and the right hemisphere of the first monkey were used to study the representation of the horizontal meridian (three hemispheres in total). The dark blue dots in Figure 1 indicate all saccades contraversive to these three hemispheres that the two monkeys executed. A third monkey executed 74, 74, 65, and 63 upward vertical saccades of 5°, 10°, 15°, and 30° in amplitude, respectively, followed by 105, 81, 63, and 62 downward vertical saccades of 5°, 10°, 15°, and 30° in amplitude, respectively (Fig. 1, blue dots). Both hemispheres of this animal were used to study the representation of the vertical meridian. A fourth monkey executed 119 up–left oblique saccades (135° direction) of 20° amplitude and was allowed to return to the fixation point as soon or as late as she wanted within the intertrial interval and via whatever intermediate point(s) of fixation she preferred. Its contralateral (right) hemisphere was used to study the representation of oblique up saccades to visual targets. For the same reason, only the left hemisphere was used from the fifth monkey, which executed 212 down–right oblique saccades (315° direction) of 10° amplitude and was allowed to return to the fixation point at any time and by any combination of movements within the intertrial interval. The latter two monkeys, which performed saccades of only one direction, executed a combination of saccades during the intertrial period, to finally return to straight ahead. The return saccades of these two animals were not focused enough in oculomotor space to allow their topographic representation in periarcuate space. Therefore, the two hemispheres, contralateral to the return saccades of these two monkeys, will not be further considered. The sixth monkey executed a sequence of a 20° up–left saccade (135° in direction) followed by two down–right (315° direction) 10° saccades. During the critical 10 first minutes of the experiment, this monkey performed 130 oblique up saccades and 331 oblique down saccades. The seventh monkey had to perform a sequence of two 10° up–left saccades followed by 20° down–right saccades; it executed 323 oblique up and 156 oblique down saccades. These two monkeys contributed two hemispheres contralateral to oblique

up, and two hemispheres contralateral to oblique down saccades to visual targets. Thus, we ended with three hemispheres contralateral to oblique up saccades and another three hemispheres contralateral to oblique down saccades to visual targets. All saccades executed in the 10 critical first minutes of the experiment, including task-related, fixation, and spontaneous, contraversive to the former (latter) are collectively depicted as green dots (red dots) in Figure 1.

To reveal effects induced by visually guided saccades, glucose utilization values obtained from monkeys executing saccades were compared with those obtained from the two hemispheres of a monkey that was seated in the dark (Cd) in front of the idle apparatus and received reward at random intervals, to match the average number of rewards received by monkeys executing saccades. Saccades executed by the Cd monkey in the critical 10 first minutes of the experiment are collectively depicted as black dots in Figure 1. Finally, to disambiguate the effect of large visually guided saccades from that of target fixation and small fixation saccades, the activation of the periarcuate cortex of monkeys executing saccades to visual targets was compared with that of two fixation-control (Cf) monkeys (four hemispheres). These animals maintained fixation of a central visual target located straight ahead for 75% of the duration of the ^{14}C-DG experiment.

Quantitative Cortical Maps
The As was analyzed in the 17 hemispheres described earlier, each extending through ~750, 20 μm thick, serial horizontal sections. One section every 10–25 (depending on the region studied) was stained with thionin to identify cytoarchitectonically cortical areas of interest, using the criteria of Petrides and Pandya (1999), (2002) for the prearcuate cortex, and Matelli and colleagues (Matelli et al. 1991; Geyer et al. 2000) for the postarcuate cortex. Cytoarchitectonic characteristics in the area around the fundus were distorted in our horizontal sections due to the geometry of the sulcus. This area is marked as 44 based on previous studies. In all hemispheres, we excluded the ventralmost sections through the arcuate (covering the ventralmost 4 mm of the sulcus) since this granular cortex is now considered an area separate from area 6 (Preuss and Goldman-Rakic 1991; Petrides et al. 2005; Belmalih et al. 2009). Figure 4A shows the quantitative 2D map of the spatio-intensive distribution of metabolic activity (as LCGU values in

micromoles/100 g/minute) within arcuate and prearcuate cortical areas, averaged from the two hemispheres of the control monkey in the dark (Cd). In this and the following figures, the reconstructions of both hemispheres are printed following the same convention, namely anterior is left and posterior is right. Figure 4B also shows a quantitative map of the spatial distribution of metabolic activity, this time averaged from all remaining hemispheres (15), contralateral to the clouds of horizontal, oblique (upward and downward), and vertical saccades, and also including the four hemispheres of the fixation monkeys. To visualize the net visuomotor activation quantitatively, we subtracted the map shown in Figure 4A from the map shown in Figure 4B. The resulting image is shown in Figure 4C and demonstrates that visually guided saccades activate (1) areas 8A and 45 of the anterior bank of the As and the prearcuate convexity, (2) the cortex around the fundus of the As including area 44 (Petrides et al. 2005; Belmalih et al. 2009), and (3) area 6 of the posterior bank of the As particularly the part lying in the ventral limb of the As (i.e. area F5 [Matelli et al. 1985; Geyer et al. 2000]), whereas it spares area 8B.

A comparison of the average map obtained from monkeys performing contraversive downward oblique saccades to visual targets (Fig. 5A) with the average Cd map (Fig. 4A) demonstrates that oblique downward saccades activate mostly the dorsal part of the periarcuate cortex overlying area 8A in the anterior bank of the As and the adjacent cortex at the fundus of the sulcus including area 44 as well as the prearcuate convexity. The effect becomes more evident when all pixels with LCGU values higher by at least 10% over those of the corresponding Cd map are marked (in red) as is the case in Figure 6A. Conversely, the quantitative map of LCGU values averaged from the hemispheres of monkeys executing contraversive upward oblique saccades to visual targets (Figs 5B and 6B) demonstrates that these are represented more ventrally, that is, in area 45 of the anterior bank of the As and the prearcuate convexity, in the ventral part of the cortex straddling the fundus of the As (including area 44) and in the posterior bank of the As. To illustrate the representation of the horizontal meridian, we averaged the quantitative metabolic maps obtained from the hemispheres contralateral to horizontal saccades. As shown in Figure 5C, this is represented as a strip of cortex close to the middle of the map, running from the posterior crown of the As through its posterior bank, the fundus, the anterior bank close to the border between areas 45 and 8A and continues rostrally through the prearcuate convexity. This is particularly clear when pixels with LCGU values of >10% over those of the corresponding Cf map are marked (in blue in Fig. 6C). The same pattern emerged when the Cd was used instead, but use of the Cf was dictated by the relatively long periods of time the subjects spent fixating the targets. Finally, the representation of the vertical meridian, generated from the hemispheres of the monkey executing vertical saccades (both upward and downward) to visual targets, is shown as a quantitative metabolic map in Figure 5D, and as a map of LCGU values of >10% relative to Cf in Figure 6D. As shown here, the representation of the vertical meridian runs parallel to the posterior border of areas 8A and 45 and the ventral border of area 8B. Since most fixation neurons of the FEF are found in an area corresponding to the foveal representation of the FEF (Izawa et al. 2009), it is reasonable to expect the intersection of the horizontal and vertical meridians (Fig. 6E) to lie close to the representation of miniscule saccades such as those executed by

the Cf monkey. Indeed, the region more intensely activated in the Cf monkey, the dorsalmost 5 mm of the inferior ramus of the As close to the fundus of the sulcus (Moschovakis et al. 2004), agrees well with the herein demonstrated location of the intersection of the two meridians. This region displayed a LCGU value equal to 66.8 μmol/100 g/min when averaged across all monkeys executing visually guided saccades and a value of 64.7 μmol/100 g/min when averaged across the Cf monkeys. These values, sampled within the fixation-related area, are significantly higher (by 19% and 15%, respectively) than the corresponding value in the Cd monkey (56.3 μmol/100 g/min).

In each group of monkeys executing saccades, we measured the average LCGU values in the four periarcuate subregions representing (1) the horizontal meridian, (2) the vertical meridian, (3) oblique upward, and (4) oblique downward saccades to visual targets (shown in different colors in Fig. 6) and we compared them with the corresponding averaged Cf values as well as with the corresponding Cd values (Table 2). Because the intensity of the saccade-related activation was not the same in all hemispheres, nor was the number of saccades toward a target the same for all animals, we examined whether the number of saccades executed is correlated with increased activation (relative to the Cf and Cd values). Figure 7 illustrates a 2D graph of the increased glucose consumption (percent LCGU difference relative to Cf) versus the number of movements, separately for the different subregions of the periarcuate cortex (marked in red, green, dark blue, and light blue in Fig. 6). For example, three of the data points reflect the number of contraversive oblique upward saccades plotted against the average %LCGU-dif found in the region representing the upper visual space in each of the three relevant hemispheres. The relatively high value of the correlation coefficient (0.83) is indicative of the fairly tight linear relationship of the two variables ($P < 0.002$). The correlation was virtually the same whether the map lying in front ($r = 0.84$, $P < 0.001$) or behind ($r = 0.80$, $P < 0.003$) the fundus of the As was considered alone. Correlations are similar when the Cd animal is considered instead (rostral map: $r = 0.76$, $P < 0.006$; caudal map: $r = 0.79$, $P < 0.004$). In contrast to our previous observations regarding the saccade-related activation of the intraparietal sulcus (Savaki et al. 2010), the slope of the relationships in the As is rather steep as an almost 4-fold difference in behavior

$$y = 0.054x + 0.006$$
$$r = 0.83$$
$$p < 0.002$$
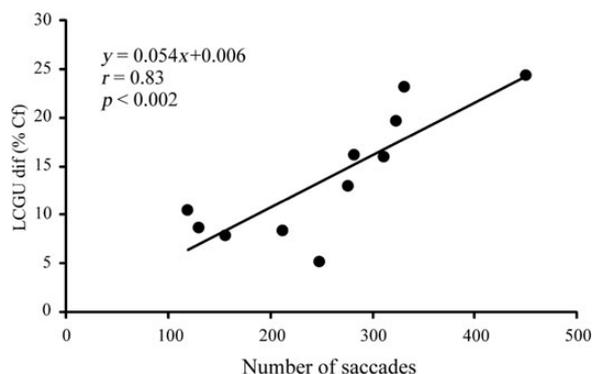
Figure 7. Two-dimensional plot of the number of contraversive visually guided saccades (abscissa) versus increase in glucose consumption relative to the fixating monkey (LCGU-dif, %Cf) in different subregions of the periarcuate cortex (ordinate). Each data point is from a different hemisphere. The solid line is the linear regression line through the data and obeys the equation displayed.

(the range of number of saccades: 119–450) leads to an almost 500% change in glucose consumption (the range of percentage LCGU difference: 5.2–24.4%). On the other hand, the number of ipsiversive saccades executed toward visual targets in the ipsilateral hemi-field was not correlated with glucose consumption (percent LCGU difference relative to the Cf and Cd animals), as indicated by the lack of significant correlation between the two variables ($P = 0.179$ for Cf and $P = 0.115$ for Cd, respectively).

Discussion

Our study is the first to provide maps of the representation of visual space and saccade direction in the periarcuate frontal cortex of rhesus monkeys executing saccades to visual targets. We found two such maps: the first one occupied areas 8A and 45 in the anterior bank of the As and the prearcuate convexity whereas the second one straddled the fundus of the As and extended into area 6-ventral. These two topographic maps of contraversive saccades to visual targets were separated by a region representing the vertical meridian running along the posterior borders of areas 8A and 45. The representation of the horizontal meridian runs from the caudal tip of the posterior bank of the As through its fundus, the anterior bank, and the prearcuate convexity near the border between areas 8A and 45 until the anterior border of area 8A. It separates regions related to upward (represented ventrolaterally) from regions related to downward (represented dorsomedially) saccades to visual targets.

Cautionary Remarks

Before we discuss our findings in the context of previous work, we wish to emphasize an important potential limitation arising from the fact that the FEF can be activated both by visual stimuli and eye movements. Given that saccade-related FEF neurons discharge much more intensely for saccades directed to a target, real or remembered (Goldberg and Bushnell 1981; Bruce and Goldberg 1985), we chose the presentation of visual targets as the most effective means to drive the regions we wanted to study. Since we also wished to distinguish activations due to presaccadic discharges from those due to visual responses and to reconstruct a map of oculomotor rather than a map of visual space, two additional monkeys were rewarded for executing learned saccades of more or less specific amplitudes and directions on auditory cue and in the absence of a target. Although the activation of the periarcuate cortex of these two monkeys was increased relative to the Cd, the increase was modest (∼7%, i.e., at the limit of statistical significance of the technique). The modest activations we observed for learned saccades could be due to the washing out of any effects due to the diffuse engagement of the periarcuate eye fields. In turn, this could be due to the fact that the end points of learned saccades executed on cue were spread out much more broadly than those of saccades to visual targets (Bakola et al. 2007; Savaki et al. 2010). It could also be due to the fact that movement cells of the As are less sharply tuned to direction and amplitude than visuomovement cells and these in turn are less sharply tuned than visual cells (Bruce and Goldberg 1985).

On the other hand, the modest activation of the periarcuate cortex for learned saccades contrasts our findings in the

intraparietal area and the superior temporal sulci of the same monkeys (Bakola et al. 2006, 2007), possibly due to differences in the discharges of the relevant cells of these areas. For example, whereas movement cells of the FEF discharge as briskly for learned and visually guided saccades, the visuomovement cells that are about twice as numerous often discharge less or much less for learned saccades (Bruce and Goldberg 1985). This is not the case for LIP neurons, which "have an independent presaccadic activation that is unrelated to the recent presentation of a visual stimulus" (Colby et al. 1996). However, extracellular recording data should be used with caution to explain the results obtained with an imaging technique, such as the one of the present report, given the considerable methodological differences between the studies in question. For example, the learned saccades of Bruce and Goldberg (1985) and Colby et al. (1996) were saccades directed to a target that was present on previous trials of the same session, whereas the learned saccades in our experiments were saccades directed to targets that the animal had not seen in several months.

Finally, the FEF is known to contain cells discharging before ipsiversive saccades (Crapse and Sommer 2009). Although it has been argued that such cells are probably not numerous based on the fact that one needs to lesion fairly large portions of the FEF before the reaction time of ipsiversive saccades is affected (Peel et al. 2014), the existence of such neurons could complicate the interpretation of our results since the pattern of activations we observed in one hemisphere would reflect not only the execution of contraversive saccades but also those of ipsiversive as well, in particular since the metrics (amplitude and direction) of the two were designed to differ. Additionally, ∼20% of the presaccadic cells of the FEF discharge before saccades in one direction (contraversive up or down) and after saccades of the opposite direction (Bruce and Goldberg 1985). To address these issues, two of our monkeys were instructed to generate saccades in only one direction (20° up left and 10° down right, respectively) and return to straight ahead through whatever trajectory they wished. Indeed, these two monkeys executed a combination of return saccades that were too varied to allow their topographic representation in the contralateral periarcuate cortex. Accordingly, their execution cannot have influenced much the pattern of activations we observed in the periarcuate cortex of the opposite side. It is reassuring that the pattern of activations of the periarcuate cortex of these two monkeys did not differ qualitatively from those of the monkeys executing contraversive and ipsiversive oblique saccades. Nor was the number of visually driven ipsiversive saccades correlated with glucose consumption (percent LCGU difference relative to the Cf and Cd animals). However, the representation of both ipsiversive and contraversive saccades in the periarcuate cortex might lower the signal-to-noise ratio of our technique and thus lead us to underestimate the effects we observed. Accordingly, the differences between the maps of upper and lower field representations could be stronger and the topography of visually driven saccades in the periarcuate cortex crisper than Figure 6 would have us believe.

Extent of the Periarcuate Eye Fields

The location of the classical FEF was specified with the help of electrical microstimulation. Early studies (Robinson and Fuchs 1969) described the periarcuate eye fields as fairly extensive,

encompassing the As and the exposed prearcuate convexity between the posterior angle of the As, its superior ramus, and the principal sulcus. However, these early studies made use of high-intensity currents, sometimes as high as 2 mA. A smaller, low-threshold FEF was defined later (Bruce et al. 1985). Its electrical stimulation consistently elicited saccades in response to weaker stimuli (50 micro-amperes or even lower) and is presumably co-extensive with the parts of areas 8A and 45 of Walker (Walker 1940) that contain relatively large numbers of big layer V pyramidal cells (Stanton et al. 1989). More recently, we combined the trans-synaptic transport of a retrograde tracer (rabies virus) from a single extraocular muscle (the lateral rectus) with saccade-related 2-DG functional imaging to demonstrate that the periarcuate eye fields extend beyond this relatively small region of cortex into premotor area 6 (Moschovakis et al. 2004), a finding that was later confirmed by others (Koyama et al. 2004; Baker et al. 2006). The present report also confirms this more extensive periarcuate eye field, in that it shows saccade-related activations occupying a large contiguous region of the frontal cortex within both banks of the As and the exposed convexity in front of it. However, the present study indicates a more modest involvement of area F2, in the spur and the caudal bank of the superior limb of the As, than previously suggested (Moschovakis et al. 2004). This could be due to the fact that, as shown earlier (Baker et al. 2006), saccade-related activation of the caudal bank of the As can be considerable in some subjects and absent in other.

We do not wish to imply that the periarcuate eye field of the present study is devoted exclusively to visually guided saccades. In fact, there is considerable evidence to indicate that this is unlikely to be the case. For example, a region of the posterior bank of the As near the representation of small size saccades, and the confluence of the horizontal and vertical meridians of the present study, has been implicated in smooth pursuit eye movements (Bruce et al. 1985; MacAvoy et al. 1991; Gottlieb et al. 1993; Fukushima et al. 2002; Tanaka and Lisberger 2002). It also contains cells discharging in relation to saccades and to eye position (Tanaka and Lisberger 2002), and besides impairing smooth pursuit, its inactivation disables VOR suppression in monkeys (Fukushima 1997). More rostrally, a region of the dorsolateral prefrontal cortex, bounded by the As caudally and the caudal tip of the principal sulcus rostrally, contains cells active during the verging, diverging, and accommodative movements accompanying far and near viewing, whereas its electrical stimulation has been shown to evoke convergent eye movements and ocular accommodation (Gamlin and Yoon 2000). Moreover, some neurons in the FEF encode the location of behaviorally relevant stimuli and have been implicated in attentional mechanisms distinct from those controlling saccades (Schall 2002; Thompson et al. 2005; Noudoost and Moore 2011; Gregoriou et al. 2012). Finally, we cannot exclude the possibility that large tracts of the arcuate cortex including the fundus of the As and its posterior bank are involved in coordinating the movements of the eyes with those of other effectors (e.g. eye lids, head, and arm). Indeed, some of the caudal bank of the As is thought to participate in the control of blinking movements (Bruce et al. 1985) or eye–arm coordination (Fujii et al. 2000).

Visuomotor Topography in the Frontal and Premotor Eye Fields

Presaccadic neurons of the primate FEF discharge maximally for saccades of particular metrics and less intensely for saccades of other amplitudes and directions (Bruce and Goldberg 1985). If these neurons were arranged in an orderly fashion, movement metrics would also be represented topographically in the arcuate eye fields. Indeed, corticotectal neurons are arranged topographically such that neurons discharging for small saccades are located ventrally and laterally whereas cells discharging for large saccades are located dorsally and medially in the central FEF (Bruce et al. 1985; Sommer and Wurtz 2000). Our study did not allow us to replicate these results as we did not explore systematically the effect of size upon the spread of activation in the FEF. Instead, we focused on the representation of directions of saccades to visual targets. As shown in Figure 6E, which summarizes our findings, down is represented medially (mainly in area 8A) in the FEF and up is represented laterally (mainly in area 45) and these two regions are separated by the representation of the horizontal meridian. The representation of the vertical meridian runs along the caudal border of areas 8A and 45, separating the FEF from a second map of visuo-oculomotor space that corresponds to the premotor eye field. The latter overlies part of area 44 and 6 in the caudal bank of the As. In it, downward and upward movements to visual targets are again represented dorsally and ventrally, respectively, the two representations being again separated by that of the horizontal meridian.

Although previous publications do not offer as clear a description of the representation of visuo-oculomotor space in the frontal and premotor eye fields, they contain information consistent with it. For example, Figure 9 of Bruce and Goldberg (1985) illustrates the direction of saccades evoked through electrical stimulation of sites along a track through the FEF (track A). Saccade directions are downward for superficial sites of stimulation, then horizontal near the middle of the track, and become progressively more upward the deeper into the cortex the electrode penetrates. Also, labeling of the FEF following tracer injection in the primate V4 indicates that projections from the representation of the upper field in V4 tend to be located more ventrally in the FEF than those from the representation of the lower field in V4 (Ungerleider et al. 2008). Moreover, the caudal LIP, which preferentially represents downward saccades (Savaki et al. 2010), has been shown to project to area 8A in the monkey (Section 1 of Fig. 13 of [Schall et al. 1995]), whereas the rostral LIP, which preferentially represents upward saccades (Savaki et al. 2010), has been shown to project to area 45 in the monkey (Section 3 of Fig. 13 of [Schall et al. 1995]). Actually, the fit between our data and the earlier description of anatomical LIP projections to the AS may be even closer; the dorsal portion of rostral ventral LIP (rostral LIPv), which represents upward saccades (Fig. 10 of [Savaki et al. 2010]) has been shown to project to area 45 and the ventral portion of rostral LIPv to area 8A (Section 3 of Fig. 12 of [Schall et al. 1995]). Finally, consistent with our results, Figure 6B of Suzuki and Azuma (1983) illustrates the receptive fields of six neurons located in front of the inferior limb of the AS; with one exception (cell 6 recorded along the dorsal most track behind the caudal tip of the principal sulcus), they were all almost entirely confined to the subject's upper visual field.

Finally, it is important to examine whether the herein demonstrated representation of saccade directions in the periarcuate eye fields fits the earlier demonstration that large to small saccades are represented in the FEF on a dorsoventral axis running along the As. For example, Figure 8 of Bruce et al. (1985) shows that large amplitude saccades are represented

dorsomedially and small saccades ventrolaterally. This pattern for amplitude representation is confirmed in Dias and Segraves 1999 and Figure 11 of Sommer and Wurtz 2000. Unfortunately, with the exception of Sommer and Wurtz (2000), considered in some detail later, earlier workers did not provide a sufficient number of data points to allow a direct comparison of their representation of direction or amplitude with our map. Moreover, the ambiguity of the penetration angle in the examples of Bruce et al. 1985 makes it even harder to interpret their results in light of our findings. The area studied by Sommer and Wurtz occupies the central portion of our map (Fig. 6E) where there are overlaps between green (Fig. 6A), red (Fig. 6B), dark blue (Fig. 6C), and light blue (Fig. 6D). In other words, this region of our map contains neurons responding to upward, downward, horizontal, and vertical saccades, with small saccades represented in the depth of the anterior bank of the As (around the intersection of the herein demonstrated representation of the horizontal and vertical meridians). Interestingly, in certain parts of the map, the overlap is such that one would be likely to encounter all different directions along a penetration orthogonal to the dorsoventral axis of the brain (this would run parallel to the rostrocaudal axis of our maps and would coincide with the crown to fundus trajectory of electrode penetrations at least for the portion of our maps that belongs to the anterior bank of the AS). Moreover, in penetrations such as those shown by Sommer and Wurtz, one would indeed encounter larger amplitude saccades near the crown of the AS and smaller amplitude saccades deeper in the sulcus. The major difference between the present study and that of Sommer and Wurtz is the size of the area studied by these earlier authors (originally shown in their Figs. 8 and 11B), which is much smaller (46 mm^2), that is, about one-fifth of the area found activated in our maps (220 mm^2). Given that the area we studied is much bigger than that disclosed by the electrophysiological studies mentioned earlier, we believe that our data offer a more comprehensive account of space representation in the periarcuate cortex. Neuroimaging studies are better suited to answer questions about how space is mapped onto the surface of the cortex, because they avoid the complex task of reconstructing the relationship of data points obtained from different tracks on different dates. They also have the advantage of establishing direct correspondence with neuroanatomy. Our results complement rather than contradict previously available evidence and together with experiments designed to furnish evidence about the representation of saccade size they could constitute important stepping stones in our effort to clarify how the metrics of visuo-oculomotor space are represented in the extended periarcuate eye fields.

Does the Periarcuate Eye Field Comprise one or two Maps?

The present report further demonstrates that the periarcuate eye fields we describe can in fact be split into two: a rostral one overlying areas 8A and 45 in the rostral bank of the As and the prearcuate frontal convexity and a second, caudal one, occupying area 44 and the caudal bank of the As. We wish here to examine whether this choice is consistent with recent decisions to confer the status of an area on a cortical region. Alarmed, in part, by their multiplication, Semir Zeki proposed the following criteria for separating a visual area in the cortex: (1) It should have an independent and more or less complete map of the contralateral visual field, to include

both the upper and lower quadrants. (2) Identifiable and unique functional properties. (3) A distinct set of anatomical connections. (4) A distinctive architecture (Sereno and Allman 1991; Zeki 2003).

Consistent with the first criterion, the herein demonstrated existence of two complete maps of contralateral visuo-oculomotor space in and near the primate As argues in favor of two arcuate eye fields rather than a single extended one. Two eye fields were also found in fMRI studies of the dorsolateral frontal cortex of human subjects performing saccades (Amiez et al. 2006; Kastner et al. 2007). In humans, these areas are not contiguous. One, found in the ventral branch of the superior precentral sulcus, has been consistently reported as activated for saccades in human neuroimaging studies (Paus et al. 1993; Petit et al. 1996, 1997; Doricchi et al. 1997; Culham et al. 1998) and is generally thought to correspond to the primate FEF. The second, a more recent discovery (Amiez and Petrides 2009), is located in the dorsal branch of the inferior precentral sulcus and is thought to correspond to the caudal, premotor FEF of this and our previous study (Moschovakis et al. 2004).

Consistent with the second criterion, the subsection titled "Extent of the periarcuate eye fields" (above) summarizes some of the differences between the frontal and the premotor eye fields. Whereas the former have been traditionally thought to comprise the low-threshold FEF, the posterior bank of the AS has been implicated in forelimb movements (Gregoriou and Savaki 2003; Raos et al. 2003) and in the representation of movements of the arm, hand, and mouth (Rizzolatti et al. 1988). However, the behavioral relevance of the discharge of the visuo-oculomotor cells of the premotor eye field remains unknown, and therefore, a functional distinction between the premotor and the FEFs on visuo-oculomotor grounds is uncertain.

Further, the oculomotor-related anatomical projections of the anterior bank of the As differ considerably from those of the posterior. Those of the former include the mesencephalic reticular formation, the intermediate gray layer of the superior colliculus, the nucleus prepositus hypoglossi, the supraoculomotor area, the nucleus reticularis tegmenti pontis, the paramedian pontine reticular formation, the interstitial nucleus of Cajal, and the nucleus raphe interpositus (Schnyder et al. 1985; Huerta et al. 1986; Stanton et al. 1988; Shook et al. 1990). On the other hand, the posterior bank of the AS projects to the paramedian pontine reticular formation and the intermediate gray layer of the superior colliculus (Leichnetz et al. 1981; Fries 1984; Schnyder et al. 1985). These relatively minor projections of the posterior bank of the As complement its considerable forelimb-related ones to the spinal cord in particular those arising from the arcuate premotor area in the dorsal part of its inferior limb (Dum and Strick 1991).

Finally, there are considerable cytoarchitectonic differences between the frontal and the premotor eye fields. There is only partial overlap between the low-threshold FEF and the two cytoarchitectonically defined regions of the anterior bank of the As, namely areas 8A and 45 of Walker (Walker 1940). The former occupies the dorsal half of the anterior wall of the superior limb of the As and the exposed surface close to it (Walker 1940). More recently, it was subdivided into area 8Ac located inside the bank of the As and area 8Ar on the exposed surface (Preuss and Goldman-Rakic 1991). Area 45 occupies the rostral bank of the inferior limb of the As (Walker 1940) and was also more recently subdivided into area 45b near the

fundus and area 45a near the crown (Preuss and Goldman-Rakic 1991). Areas 45 and 8A have a well-developed layer IV, densely packed with small cells, whereas ventral area 6 is essentially agranular. Area 44, which lies in between the ventral area 6 and area 45, has an irregular layer IV and is therefore considered dysgranular. The other cytoarchitectonic characteristic that distinguishes area 45 from ventral area 6 is the relative size of pyramidal cells in layers III and V. Area 45 has very large neurons in lower layer III much larger than the pyramids of layer V (Petrides et al. 2005).

To conclude, our study confirms that the caudal bank of the As, which belongs to the premotor cortex, is activated for visually guided saccades and demonstrates that the frontal and premotor eye fields represent the direction of saccades and visual targets, spatially, in an orderly fashion. The behavioral relevance of the discharge of the visuo-oculomotor cells contained in the premotor eye field remains unknown and should be the object of single unit studies.

Notes

References

Amiez C, Kostopoulos P, Champod AS, Petrides M. 2006. Local morphology predicts functional organization of the dorsal premotor region in the human brain. J Neurosci. 26:2724–2731.

Amiez C, Petrides M. 2009. Anatomical organization of the eye fields in the human and non-human primate frontal cortex. Prog Neurobiol. 89:220–230.

Baker JT, Patel GH, Corbetta M, Snyder LH. 2006. Distribution of activity across the monkey cerebral cortical surface, thalamus and midbrain during rapid, visually guided saccades. Cereb Cortex. 16:447–459.

Bakola S, Gregoriou GG, Moschovakis AK, Raos V, Savaki HE. 2007. Saccade-related information in the superior temporal motion complex: quantitative functional mapping in the monkey. J Neurosci. 27:2224–2229.

Bakola S, Gregoriou GG, Moschovakis AK, Savaki HE. 2006. Functional imaging of the intraparietal cortex during saccades to visual and memorized targets. NeuroImage. 31:1637–1649.

Belmalih A, Borra E, Contini M, Gerbella M, Rozzi S, Luppino G. 2009. Multimodal architectonic subdivision of the rostral part (area F5) of the macaque ventral premotor cortex. J Comp Neurol. 512:183–217.

Bruce CJ, Goldberg ME. 1985. Primate frontal eye fields. I. Single neurons discharging before saccades. J Neurophysiol. 53:603–635.

Bruce CJ, Goldberg ME, Bushnell MC, Stanton GB. 1985. Primate frontal eye fields. II. Physiological and anatomical correlates of electrically evoked eye movements. J Neurophysiol. 54:714–734.

Colby CL, Duhamel JR, Goldberg ME. 1996. Visual, presaccadic, and cognitive activation of single neurons in monkey lateral intraparietal area. J Neurophysiol. 76:2841–2852.

Crapse TB, Sommer MA. 2009. Frontal eye field neurons with spatial representations predicted by their subcortical input. J Neurosci. 29:5308–5318.

Culham JC, Brandt SA, Cavanagh P, Kanwisher NG, Dale AM, Tootell RB. 1998. Cortical fMRI activation produced by attentive tracking of moving targets. J Neurophysiol. 80:2657–2670.

Dias EC, Segraves MA. 1999. Muscimol induced inactivation of monkey frontal eye field: effects on visually and memory guided saccades. J Neurophysiol. 81:2191–2214.

Doricchi F, Perani D, Incoccia C, Grassi F, Cappa SF, Bettinardi V, Galati G, Pizzamiglio L, Fazio F. 1997. Neural control of fast-regular saccades and antisaccades: an investigation using positron emission tomography. Exp Brain Res. 116:50–62.

Dum RP, Strick PL. 1991. The origin of corticospinal projections from the premotor areas in the frontal lobe. J Neurosci. 11:667–689.

Fries W. 1984. Cortical projections to the superior colliculus in the macaque monkey: a retrograde study using horseradish peroxidase. J Comp Neurol. 230:55–76.

Fujii N, Mushiake H, Tanji J. 1998. An oculomotor representation area within the ventral premotor cortex. Proc Natl Acad Sci. 95:12034–12037.

Fujii N, Mushiake H, Tanji J. 2000. Rostrocaudal distinction of the dorsal premotor area based on oculomotor involvement. J Neurophysiol. 83:1764–1769.

Fukushima K. 1997. Corticovestibular interactions: anatomy, electrophysiology, and functional considerations. Exp Brain Res. 117:1–16.

Fukushima K, Yamanode T, Shinmei Y, Fukushima J, Kurkin S, Peterson BW. 2002. Coding of smooth eye movements in three-dimensional space by frontal cortex. Nature. 419:157–162.

Gamlin PD, Yoon K. 2000. An area for vergence eye movement in primate frontal cortex. Nature. 407:1003–1007.

Geyer S, Matelli M, Luppino G, Zilles K. 2000. Functional neuroanatomy of the primate isocortical motor system. Anat Embryol. 202:443–474.

Goldberg ME, Bushnell MC. 1981. Behavioral enhancement of visual responses in monkey cerebral cortex. II. Modulation in frontal eye fields specifically related to saccades. J Neurophysiol. 46:773–787.

Gottlieb JP, Bruce CJ, MacAvoy MG. 1993. Smooth eye movements elicited by microstimulation in the primate frontal eye field. J Neurophysiol. 69:786–799.

Gregoriou GG, Gotts SJ, Desimone R. 2012. Cell-type-specific synchronization of neural activity in FEF with V4 during attention. Neuron. 73:581–594.

Gregoriou GG, Luppino G, Matelli M, Savaki HE. 2005. Frontal cortical areas of the monkey brain engaged in reaching behavior: a (14) C-deoxyglucose imaging study. NeuroImage. 27:442–464.

Gregoriou GG, Savaki HE. 2001. The intraparietal cortex: subregions involved in fixation, saccades, and in the visual and somatosensory guidance of reaching. J Cereb Blood Flow Metab. 21:671–682.

Gregoriou GG, Savaki HE. 2003. When vision guides movement: a functional imaging study of the monkey brain. NeuroImage. 19:959–967.

Huerta MF, Krubitzer LA, Kaas JH. 1986. Frontal eye field as defined by intracortical microstimulation in squirrel monkeys, owl monkeys, and macaque monkeys: I. Subcortical connections. J Comp Neurol. 253:415–439.

Izawa Y, Suzuki H, Shinoda Y. 2009. Response properties of fixation neurons and their location in the frontal eye field in the monkey. J Neurophysiol. 102:2410–2422.

Kastner S, DeSimone K, Konen CS, Szczepanski SM, Weiner KS, Schneider KA. 2007. Topographic maps in human frontal cortex revealed in memory-guided saccade and spatial working-memory tasks. J Neurophysiol. 97:3494–3507.

Kennedy C, Sakurada O, Shinohara M, Jehle J, Sokoloff L. 1978. Local cerebral glucose utilization in the normal conscious macaque monkey. Ann Neurol. 4:293–301.

Koyama M, Hasegawa I, Osada T, Adachi Y, Nakahara K, Miyashita Y. 2004. Functional magnetic resonance imaging of macaque monkeys performing visually guided saccade tasks: comparison of cortical eye fields with humans. Neuron. 41:795–807.

Leichnetz GR, Spencer RF, Hardy SG, Astruc J. 1981. The prefrontal corticotectal projection in the monkey; an anterograde and retrograde horseradish peroxidase study. Neuroscience. 6:1023–1041.

MacAvoy MG, Gottlieb JP, Bruce CJ. 1991. Smooth pursuit eye movement representation in the primate frontal eye field. Cereb Cortex. 1:95–102.

Matelli M, Luppino G, Rizzolatti G. 1991. Architecture of superior and mesial area 6 and the adjacent cingulate cortex in the macaque monkey. J Comp Neurol. 311:445–462.

Matelli M, Luppino G, Rizzolatti G. 1985. Patterns of cytochrome oxidase activity in the frontal agranular cortex of the macaque monkey. Behav Brain Res. 18:125–136.

Moschovakis AK, Gregoriou GG, Savaki HE. 2001. Functional imaging of the primate superior colliculus during saccades to visual targets. Nat Neurosci. 4:1026–1031.

Moschovakis AK, Gregoriou GG, Ugolini G, Doldan M, Graf W, Guldin W, Hadjidimitrakis K, Savaki HE. 2004. Oculomotor areas of the primate frontal lobes: A transneuronal transfer of rabies virus and [14C]-2-Deoxyglucose functional imaging study. J Neurosci. 24:5726–5740.

Moschovakis AK, Scudder CA, Highstein SM. 1996. The microscopic anatomy and physiology of the mammalian saccadic system. Progr Neurobiol. 50:133–524.

Noudoost B, Moore T. 2011. Control of visual cortical signals by prefrontal dopamine. Nature. 474:372–375.

Paus T, Petrides M, Evans AC, Meyer E. 1993. Role of the human anterior cingulate cortex in the control of oculomotor, manual, and speech responses: a positron emission tomography study. J Neurophysiol. 70:453–469.

Peel TR, Johnston K, Lomber SG, Corneil BD. 2014. Bilateral saccadic deficits following large and reversible inactivation of unilateral frontal eye field. J Neurophysiol. 111:415–433.

Petit L, Clark VP, Ingeholm J, Haxby JV. 1997. Dissociation of saccade-related and pursuit-related activation in human frontal eye fields as revealed by fMRI. J Neurophysiol. 77:3386–3390.

Petit L, Orssaud C, Tzourio N, Crivello F, Berthoz A, Mazoyer B. 1996. Functional anatomy of a prelearned sequence of horizontal saccades in humans. J Neurosci. 16:3714–3726.

Petrides M, Cadoret G, Mackey S. 2005. Orofacial somatomotor responses in the macaque monkey homologue of Broca's area. Nature. 435:1235–1238.

Petrides M, Pandya DN. 2002. Comparative cytoarchitectonic analysis of the human and the macaque ventrolateral prefrontal cortex and corticocortical connection patterns in the monkey. Eur J Neurosci. 16:291–310.

Petrides M, Pandya DN. 1999. Dorsolateral prefrontal cortex: comparative cytoarchitectonic analysis in the human and the macaque brain and corticocortical connection patterns. Eur J Neurosci. 11:1011–1036.

Preuss TM, Goldman-Rakic PS. 1991. Myelo- and cytoarchitecture of the granular frontal cortex and surrounding regions in the strepsirhine primate Galago and the anthropoid primate Macaca. J Comp Neurol. 310:429–474.

Raos V, Evangeliou MN, Savaki HE. 2007. Mental simulation of action in the service of action perception. J Neurosci. 27:12675–12683.

Raos V, Franchi G, Galesse V, Fagassi L. 2003. Somatotopic organization of the lateral part of area F2 (dorsal premotor cortex) of the macaque monkey. J Neurophysiol. 89:1503–1518.

Rizzolatti G, Camarda R, Fogassi L, Gentilucci M, Luppino G, Matelli M. 1988. Functional organization of inferior area 6 in the macaque monkey: II. Area F5 and the control of distal movements. Exp Brain Res. 71:491–507.

Robinson DA, Fuchs AF. 1969. Eye movements evoked by stimulation of frontal eye fields. J Neurophysiol. 32:637–648.

Savaki HE, Davidsen L, Smith C, Sokoloff L. 1980. Measurement of free glucose turnover in brain. J Neurochem. 35:495–502.

Savaki HE, Gregoriou GG, Bakola S, Raos V, Moschovakis AK. 2010. The place code of saccade metrics in the lateral bank of the intraparietal sulcus. J Neurosci. 30:1118–1127.

Schall JD. 2002. The neural selection and control of saccades by the frontal eye field. Philos Trans R Soc Lond B Biol Sci. 357:1073–1082.

Schall JD, Morel A, King DJ, Bullier J. 1995. Topography of visual cortex connections with frontal eye field in macaque: convergence and segregation of processing streams. J Neurosci. 15:4464–4487.

Schnyder H, Reisine H, Hepp K, Henn V. 1985. Frontal eye field projection to the paramedian pontine reticular formation traced with wheat germ agglutinin in the monkey. Brain Res. 329:151–160.

Sereno MI, Allman JM editors. 1991. Cortical Visual Areas in Mammals. City: Macmillan.

Shook BL, Schlag-Rey M, Schlag J. 1990. Primate supplementary eye field. I. Comparative aspects of mesencephalic and pontine connections. J Comp Neurol. 301:618–642.

Sokoloff L, Reivich M, Kennedy C, Des Rosiers MH, Patlak CS, Pettigrew KS, Sakurada O, Shinohara M. 1977. The [14C]-deoxyglucose method for the measurement of local cerebral glucose utilization: Theory, procedure, and normal values in the conscious and anesthetized albino rat. J Neurochem. 28:879–916.

Sommer MA, Wurtz RH. 2000. Composition and topographic organization of signals sent from the frontal eye field to the superior colliculus. J Neurophysiol. 83:1979–2001.

Sparks DL, Holland R, Guthrie BL. 1976. Size and distribution of movement fields in the monkey superior colliculus. Brain Res. 113:21–34.

Stanton GB, Deng S-Y, Goldberg ME, McMullen NT. 1989. Cytoarchitectural characteristics of the Frontal Eye Fields in Macaque monkeys. J Compar Neurol. 282:415–427.

Stanton GB, Goldberg ME, Bruce CJ. 1988. Frontal Eye Field efferents in the macaque monkey: I. Subcortical pathways and topography of striatal and thalamic fields. J Comp Neurol. 271:473–492.

Suzuki H, Azuma M. 1983. Topographic studies on visual neurons in the dorsolateral prefrontal cortex of the monkey. Exp Brain Res. 53:47–58.

Tanaka M, Lisberger SG. 2002. Role of arcuate frontal cortex of monkeys in smooth pursuit eye movements. I. Basic response properties to retinal image motion and position. J Neurophysiol. 87:2684–2699.

Thompson KG, Biscoe KL, Sato TR. 2005. Neuronal basis of covert spatial attention in the frontal eye field. J Neurosci. 25:9479–9487.

Ungerleider LG, Galkin TW, Desimone R, Gattass R. 2008. Cortical Connections of Area V4 in the Macaque. Cerebral Cortex. 18:477–499.

Walker AE. 1940. A cytoarchitectural study of the prefrontal area of the macaque monkey. J Comp Neurol. 73:59–86.

Zeki S. 2003. Improbable areas in the visual brain. Trends Neurosci. 26:23–26.